Triiodothyronine Prevents Cardiac Ischemia/Reperfusion Mitochondrial Impairment and Cell Loss by Regulating miR30a/p53 Axis

Francesca Forini, Claudia Kusmic, Giuseppina Nicolini, Laura Mariani, Riccardo Zucchi, Marco Matteucci, Giorgio Iervasi,and Letizia Pitto

Consiglio Nationale delle Ricerche (CNR) Institute of Clinical Physiology (F.F., C.K., G.N., L.M., G.I.,L.P), Via G. Moruzzi 1, Pisa, Italy; Department of Pathology (R.Z., G.I.), University of Pisa, 56127 Pisa, Italy; Scuola Superiore Sant'Anna (M.M., G.I.), Piazza Martiri della Libertà 33, Pisa, Italy; CNR/Tuscany Region G Monasterio Foundation (G.I.), Via G. Moruzzi 1, Pisa, Italy

Mitochondrial dysfunctions critically affect cardiomyocyte survival during ischemia/reperfusion (I/R) injury. In this scenario p53 activates multiple signaling pathways that impair cardiac mitochondria and promote cell death. p53 is a validated target of miR-30 whose levels fall under ischemic conditions. Although triiodothyronine (T3) rescues post-ischemic mitochondrial activity and cell viability, no data are available on its role in the modulation of p53 signaling in I/R. Here we test the hypothesis that early T3 supplementation in rats inhibits the post I/R activation of p53 pro-death cascade through the maintenance of miRNA 30a expression.

In our model, T3 infusion improves the recovery of post-ischemic cardiac performance. At the molecular level, the beneficial effect of T3 is associated with restored levels of miR-30a expression in the area at risk (AAR) that correspond to p53 mRNA downregulation. The concomitant decrease in p53 protein content reduces Bax expression and limits mitochondrial membrane depolarization resulting in preserved mitochondrial function and decreased apoptosis and necrosis extent in the AAR. Also in primary cardiomyocyte culture of neonatal rats, T3 prevents both miR-30a downregulation and p53 raise induced by hypoxia. The regulatory effect of T3 is greatly suppressed by miR-30a knockdown. Overall these data suggest a new mechanism of T3-mediated cardioprotection that is targeted to mitochondria and acts, at least in part, through the regulation of miR-30a/p53 axis.

Acute myocardial infarction (AMI) leading to ischemic heart disease is a major cause of death in Western societies. Although timely reperfusion effectively reduces short-term mortality, restoration of blood flow through the previously ischemic myocardium yields additional reperfusion injury, including cardiomyocyte (CM) dysfunction and death that in the long run prompts adverse cardiac remodeling (1, 2). As a consequence, prevention or limitation of cardiac damage in the early stages of the process is a crucial step in ameliorating patient prognosis.

Multiple lines of evidence demonstrate that mitochondrial functional impairments are critical determinants for myocyte loss during the acute ischemic stage, as well as for the progressive decline of surviving myocytes during the subacute and chronic stages (2–4). The critical mitochondrial event in apoptosis is mitochondrial outer membrane permeabilization, prompted by the proapoptotic BCl-2 family that leads to cytochrome c release and caspase activation. In contrast, the key mitochondrial event in necrosis is opening of the mitochondrial permeability transition pore in the inner membrane that dissipates inner mitochondrial membrane potential leading to ATP depletion, further reactive oxygen species production, swelling, and organelle rupture (3, 5). Propagation of the injury to

ISSN Print 0013-7227 ISSN Online 1945-7170
Printed in U.S.A.

Received February 5, 2014. Accepted July 24, 2014.

Abbreviations: Aar, area at risk; AMI, acute myocardial infarction; CM, cardiomyocyte; FT3, free T3; FT4, free T4; HF, heart failure; I/R, ischemia/reperfusion; KD, knockdown; LAD, left descending coronary artery; low-T3S, low-T3 syndrome; LV, left ventricle; LVFS, left ventricle fractional shortening; RZ, remote zone; T3, triiodothyronine; TH, thyroid hormone; TUNEL, terminal deoxynucleotide nick-end labeling.

neighboring organelles results in irreversible mitochondrial dysfunction, bioenergetic failure, and necrotic cell death (6, 7). Therefore, it would be rational to develop an effective therapeutic strategy aimed at reducing mitochondrial damage in the early phase of post-reperfusion wound healing.

miRNAs, a relatively new class of 22-nt nonprotein-coding single-strand RNAs, regulate several cellular processes of cardiac remodeling and heart failure (HF) (8–11), and have become an intriguing target for therapeutic intervention (12). Some of them have recently attracted attention as regulators of mitochondrial dynamics and mitochondrial cell death signaling in both myocardial ischemia/reperfusion (I/R) and in vitro models of oxidative stress (13–16). The miR-30 family members are abundantly expressed in the mature heart, but they are significantly dysregulated in human HF, in experimental I/R, and in vitro after oxidative stress (10, 17–18). miR-30a has been shown to target p53, a well-known activator of mitochondrial apoptosis that has recently been involved in necrotic mitochondrial pathways (16, 19, 20). Therefore, maintenance of miR-30a levels may be regarded as cardioprotective.

Thyroid hormones (THs) are well-known modulators of mitochondrial biogenesis, function, and Ca^{2+} cycling (21–23). Changes in thyroid status are associated with bioenergetic remodeling of cardiac mitochondria and profound alterations in the biochemistry of cardiac muscle, with repercussions on its structure and contractility (22). Current evidence shows that triiodothyronine (T3), the biologically active TH, significantly declines after AMI both in animal models and in patients (24–26). Also, low-T3 syndrome (low-T3S) is a strong independent prognostic predictor of death and major adverse cardiac events (27). Consistently, growing evidence suggests that hormonal treatment of low-T3S exerts cardioprotective effects in both humans and animal models (28–31).

In this study we focused on the role of miR-30a/p53 circuit in mitochondrial activity and cardiac performance in the I/R rat treated with T3 early infusion at near-physiological dose. To the best of our knowledge, our results indicate for the first time that the cardioprotective effect exerted in vivo by T3 supplementation after I/R is paralleled by the prevention of myocardial miR-30a level decrease. This action in turn limits the activation of p53 signaling critically involved in both mitochondrial impairment and cellular death pathways.

Materials and Methods

Animal procedure

Animals used in this investigation conformed to the recommendations in the Guide for the Care and Use of Laboratory Animals published by the United States National Institutes of Health (NIH Publication No. 85–23, revised 1996) and the protocol was approved by the Animal Care Committee of the Italian Ministry of Health (Endorsement n.135/2008-B). All surgery was performed under anesthesia, and all efforts were made to minimize suffering. Myocardial infarction was produced by ligation of the left descending coronary artery (LAD) of adult male Wistar rats 12- to 15-weeks-old and weighing 310 ± 3g using a technique described in detail elsewhere (18). See the Supplemental Data for additional information.

Experimental protocol

To mimic the low T3 syndrome observed in the clinical setting, only the I/R rats that exhibited a $> 50\%$ reduction of their basal serum FT3 level 24 hours after surgery were randomly treated for 48 hours with a constant subcutaneous infusion of 6 μg/kg/d T3 (I/R-T3, n = 8) or saline (I/R, n = 8) via a miniosmotic pump (Alzet, model 2ML4). A group of sham-operated rats was treated with constant infusion of saline and used as control (Sham group, n = 8).

Three days after surgery hearts were arrested in diastole by a lethal KCl injection. Cardiac tissue samples were obtained from a) the left ventricle (LV) free wall remote to LAD region (remote zone, RZ), b) the core of the ischemia-reperfused region (area at risk, AAR) of the LV, and c) the right ventricle. In sham-operated animals tissues were harvested from analogously termed corresponding regions. Part of the samples from each area were stored at −80°C until use and part of them were immediately processed for mitochondria isolation. Some additional hearts (n = 3) in each group were dedicated to for histology and immunohistochemistry and were processed as described below.

Echocardiography study

Echocardiographic studies were performed 3 days after infarction with a portable ultrasound system (MyLab 25, Esaote SpA) equipped with a high frequency linear transducer (LA523, 12.5 MHz). Images were obtained from the sedated animal, from the left parasternal view. Short-axis 2-dimensional view of the LV was taken at the level of papillary muscles to obtain M-mode recording. Anterior (ischemia-reperfused) and posterior (viable) end-diastolic and end-systolic wall thicknesses, systolic wall thickening, and LV internal dimensions were measured after the American Society of Echocardiography guidelines. Parameters were calculated as mean of the measures obtained in three consecutive cardiac cycles. The global LV systolic function was expressed as percent of fractional shortening.

Morphometric analysis to determine the area at risk and infarct size

Three days after surgery, the chest was reopened and the LAD retied with the suture left in its original position. A quantity of 1 mL 1% Evan's blue was injected in the inferior cava vein to identify the myocardial area at risk as unstained. Next, the heart was arrested in diastole by lethal KCl injection, excised, and cut in transversal and parallel slices about 2 mm thick. Fresh slices were incubated with triphenyltetrazolium chloride 1% solution at 37°C for 10 minutes to mark viable myocardium within the AAR. Viable myocardium outside the AAR was blue; viable myocardium within the AAR stained red, whereas the injured myocytes appeared negative for triphenyltetrazolium chloride.

LV area, the AAR, (expressed as percentage of the LV), and the infarcted area (expressed as percentage of AAR) from each slice were measured using Image J software.

Histology and immunohistochemistry

Thereafter, the slices were fixed in 10% buffered formalin and embedded in paraffin. Serial 5- to 7-μm transverse sections were processed for histological and immunohistochemical staining with hematoxylin-eosin and in situ terminal deoxynucleotide nick-end labeling (TUNEL, Roche Molecular Biochemicals) followed by 4′, 6-diamidino-2-phenylindole (DAPI) staining of nuclei, and alpha sarcomeric actin (1:100, Abcam) was used as CM-specific marker. Primary antibody was detected by incubating the sections with FITC-conjugated antimouse IgG (1:300, Abcam, green emission). Images were analyzed using light and fluorescent microscopy (Zeiss). TUNEL-positive (green) nuclei were counted from 10 randomly chosen microscope fields of 3 midventricular sections for each heart and were expressed as the percentage of total nuclei of CMs (both blue and green staining nuclei) from the same fields, using 3 hearts for each group.

Mitochondria isolation

Mitochondria were purified from LV fresh tissue according to the manufacturer's protocol (MITO-ISO1; Sigma) as previously described (32). Briefly, cardiac tissue was homogenized in buffer containing 10 mM HEPES, 200 mM mannitol, 70 mM sucrose, and 1 mM EGTA (PH 7.5) and centrifuged at 2000*g* at 4°C for 5 minutes. The supernatant was collected and centrifuged at 11000*g* at 4°C for 20 minutes. The pellet was suspended in storage buffer at pH 7.5 containing 10 mM HEPES, 250 mM sucrose, 1mMATP, 0.08 mM ADP, 5 mM sodium succinate, 2 mM K2HPO4, and 1 mM DTT and stored at −80°C until use. An aliquot of the suspended pellet was assayed for protein content with the BioRad protein assay kit.

Mitochondrial enzyme activity assays

Mitochondrial function was expressed as the ratio between the activity of the cytochrome *c* oxidase-1 and that of citrate synthase to correct for mitochondrial mass. Enzyme activity was assessed in 1mL cuvette by using a spectrophotometric assay kit according to the manufacturer's protocols (CYTOC-OX1, Sigma and CS0720, Sigma respectively). Measurements were run in triplicate and n ≥ 7 rats were tested in each group. See the Supplemental Data for additional information.

Measurements of superoxide in isolated mitochondria with MitoSox

Mitochondrial superoxide levels were measured in isolated mitochondria using MitoSox Red (Invitrogen), a fluorescent probe targeted to the mitochondria and specific for superoxide. Triplicate measurements were run in 96-well plates in a final 200μL volume and n = 4 rats were tested in each group. See the Supplemental Data for additional information.

Measurements of ATP production in isolated mitochondria

ATP synthesis rates were measured in mitochondrial fractions with the ATP Determination Kit A22066 (Life Technologies). The assays were performed in triplicate in 96-well plate in a volume of 150μL containing10μg mitochondrial protein, 0.25M sucrose, 50 mM HEPES, 2 mM MGCl2, 1mMEGTA, 10 mM KH2PO4, 1 mM pyruvate, 1 mM malate. 1 mM ATP-free ADP and a solution of 0.5 mM luciferin and 0.25 μg/ml luciferase were added with the injectors integrated in the plate reader (Infinite M200 PRO, TECAN). The slope of luminescence increase was determined in the first 48 seconds after injection of luciferase reagent plus ADP and it was converted to ATP concentration using a standard curve according to the manufacturer's instruction (n ≥ 4 rats in each group were tested). See Supplemental Data for additional information.

Inner mitochondrial membrane depolarization assay

Mitochondrial membrane depolarizes as a consequence of mitochondrial permeability transition. Changes in potential were analyzed in isolated mitochondria by using the 5,5′,6,6′-tetrachloro-1,1′,3,3′ tetraethylbenzimidazolylcarbocyanine iodide (JC-1) staining kit according to the manufacturer's protocol (CS0760; Sigma). Assay was performed in triplicate in 96-well plates (n ≥ 7 animals for each group). See the Supplemental Data for additional information.

Serum and tissue TH levels

A quantity of 2 mL of blood were collected from the femoral vein either before, or 1 and 3 days after LAD occlusion. Serum T3 and T4 were assayed as previously described (32). Tissue concentration of TH was determined in right ventricles that were pooled within each group according to the serum TH levels, and assessed as previously reported (33). Briefly, about 1 g of tissue was homogenized at 4°C in 1 mL of phosphate buffer (154 mM NaCl, 10 mM NaH2PO4, pH 7.4). The homogenate was centrifuged for 10 minutes at 4000 *g* in a cold room, and the supernatant was collected for the assay in a tandem mass spectrometry coupled to high performance liquid chromatography.

Cell cultures

Neonatal rat CMs were isolated from hearts of 2-to 3-day-old Wistar rats using the Worthington Neonatal Cardiomyocyte Isolation System according to the manufacturer's instructions. CM were grown in a humidified atmosphere of 5% CO2 at 37°C in DMEM-F12 with 2 mM L-glutamine, 1% penicillin and streptomycin and 10% FBS deprived of TH with standard charcoal stripping procedures (TH-free medium).

Forty-eight hours after isolation 2×10^5 cells/well were transfected in a 6-well plate via 5-hour incubation in optimem (Gibco) containing 80 nM 2′O methylated decoy rno-miR-30a or 2′O methylated control decoy (See Supplemental Table 1). Lipofectamine 2000 (Invitrogen) was used as transfectant according to the manufacturer's recommendations. Twenty-four hours after transfection CM were placed in a hypoxia chamber (Modular Incubator Chamber, Billups-Rothenberg, Inc), through which a mixture of 95% N_2 and 5% CO_2 gas was passed at 2 p.s.i. The chamber was then sealed and placed at 37°C for an additional 24 hours. After this period, cells were reoxygenated for 2 hours before being incubated with 100 nM T3 or vehicle. After 24-hour incubation, CM were harvested and stored at −80°C until use. CM transfected with control decoy and not exposed either to hypoxia or T3 treatment were used as control. Three batches of CM were isolated and tested in all culture conditions in three

different experimental sets. Cell pellets were harvested and used for the subsequent analysis.

Western blot analysis

Cardiac tissue and cells were lysed in Lysis buffer [20 mM Tris-HCl pH 8.0, 20 mM Nacl, 10% glycerol, 1% NP40, 10 mM EDTA, 2 mM PMSF, 2.5 μg/mL leupeptin, 2.5 μg/mL pepstatin]. For cardiac tissue, mechanical fragmentation by Tissuelyser (Qiagen) was also used. Proteins (30 μg per lane) were separated on 4% to 12% polyacrylamide gel (Bolt Bis Tris mini gels Life Technologies) and transferred to iBlot 0.2 μm PVDF membranes (Life Technologies). Immunoblotting of the membranes was performed with primary antibodies against p53 (1:1000, Cell Signaling) and HPRT (1:10000, Abcam). Signals were revealed after incubation with the secondary antibody coupled to peroxidase (1:3000, Cell Signaling) using the Clarity ECL Substrate (Biorad). Samples were run in duplicate. Acquired images were quantified using Optiquant software.

Real-time PCR

Total RNA was extracted from homogenized heart tissue and cell cultures with a Qiagen miRneasy mini kit (Qiagen) as directed by the manufacturers' instructions. For first-strand cDNA synthesis, 1 μg total RNA was reverse-transcribed in a 20-μL volume using the Mini Script RT II kit according to the manufacturer's instructions (Qiagen). PCR amplification was performed in triplicate in a Rotor Gene Q real time machine with 5 minutes of initial denaturation and then 40 cycles for mRNA: 95°C 10 seconds (denaturation), 58°C 20 seconds (annealing), 72°C 10 seconds (extension); and for miRNA: 95°C 15 seconds (denaturation), 55°C 30 seconds (annealing), 72°C 10 seconds (extension). The reaction mixture consisted of 3.5 μL H_2O, 0.75 μL primers (10 μM), 5 μL cDNA (2ng), and 10 μL of Quantifast SYBR Green mix (Qiagen); primer sequences are listed in Supplemental Table 1. To assess product specificity, amplicons were checked by melting curve analysis. Gene and miRNA transcript values were normalized respectively with those obtained from the amplification of HPRT and snRNA-U1. All reactions were performed in triplicate, and the relative expression was quantified with the Rotor Gene Q-Series Software.

Statistical analysis

All values are expressed as mean ± SEM. Student's *t* test was used for 2-group comparisons. Comparisons of parameters among 3 groups were analyzed by 1-way ANOVA, followed by post hoc Bonferroni correction for multiple-comparison (StatView 5.0.1). Differences were considered statistically significant at a value of $P < .05$. Linear regression analysis was performed setting statistical significance as $P < .05$ (StatView 5.0.1).

Results

Effects of T3 infusion on serum and tissue TH and on the expression of recognized T3 cardiac molecular targets

To examine the effect of surgery per se versus I/R on serum free T3 (FT3) and free T4 (FT4) concentrations, pre-surgical, baseline values were compared with 72-hour values in all groups. In addition, to define the relationships between circulating and tissue hormone levels after T3 infusion, T3 was measured in RV pools obtained at the end of the experimental protocol.

Sham surgery (sham vs baseline) did not significantly change serum TH concentrations (Table 1). On the contrary, with respect to the corresponding basal level, a significant decrease in FT3 was observed in the I/R group in the presence of unaltered FT4 (Table 1). T3 infusion induced an increase in serum FT3 paralleled by a consistent drop in FT4 (Table 1). A strong correlation was found between serum FT3 and myocardial T3, indicating that heart T3 status closely reflects the systemic one (Supplemental Figure 1A).

In order to verify the heart's sensitivity to the T3 infusion at the molecular level, we assessed the expression of some well-established TH targets, namely α- and β-myosin heavy chain and miR-208a (34), as recommended by the American Thyroid Association Guide to Investigating Thyroid Hormone Economy and Action in Rodent and Cell Models (35). As expected, T3 infusion induced a significant increase in the α- myosin heavy chain /β- myosin heavy chain mRNA ratio and restored miR-208a expression, which was significantly depressed in the I/R group. (Supplemental Figure 1, B and C). Altogether, these data confirmed the occurrence of a low-T3S in the I/R group and support the effectiveness of our T3 delivery system.

Table 1. Free TH Measured in Rat Serum Before and 72 Hours After Surgery

	FT3 basal levels (pg/mL)	FT3 final levels (pg/mL)	FT4 basal levels (pg/mL)	FT4 final levels (pg/mL)
Sham	3.4 ± 0.3	3.0 ± 0.2	14.2 ± 0.6	11.4 ± 1.4
I/R	3.4 ± 0.2	2.3 ± 0.2[a, b]	13.8 ± 1.7	11.3 ± 1.0
I/R-T3	3.2 ± 0.2	5.5 ± 0.3[a, b]	14.4 ± 0.8	3.4 ± 0.5[a, b]

n = 8.

[a] $P \leq 0.003$ vs respective, basal levels.

[b] $P \leq 0.004$ vs sham-operated.

T3 infusion improves the post-ischemic recovery of cardiac function

As a second step, we determined the effects of T3 on the post-ischemic cardiac functional parameters and chamber geometry. I/R rats exhibited a significant decrease in global and regional LV contractility as determined by decreased LV fractional shortening (LVFS) and anterior systolic wall thickening as well as a significant increase in the end systolic LV diameter (Table 2). T3 supplementation blunted the detrimental effect of I/R on systolic diameter and LV anterior contractility and was able to maintain the normal LVFS after I/R. Also, T3 induced a small but significant increase in heart rate when compared with sham animals (Table 2).

Altogether, these data reveal that T3 administration is associated with preserved chamber geometry and improves cardiac functional recovery.

T3 infusion improves the recovery of mitochondrial function and reduces CM loss

Given the important contribution of mitochondria impairment to post-ischemic cardiac dysfunction, we next explored if the protective effect of T3 was related to a better recovery of the mitochondrial activity and reduced reactive oxygen species production. In the area at risk, I/R resulted in reduced citrate synthase-corrected cytochrome *c* oxidase activity, in depressed ATP production rate and in increased superoxide level (Figure 1A–C). T3 administration provided a complete recovery of mitochondrial activity in the AAR and prevented superoxide accumulation (Figure 1, A–C). No significant differences among groups were observed in the RZ (Figure 1, A–C).

We hypothesized that the better recovery of mitochondrial function observed in the I/R-T3 group could result in a lesser extent of CM death. To investigate this aspect, histological examination was performed in a subgroup of I/R-T3 hearts and compared with the I/R hearts. T3 infusion decreased the infarct size as revealed by the reduced ischemic area/AAR ratio, (Figure 2 A–C) and reduced tunnel staining in the AAR (Figure 2D). Overall, these find-

Table 2. In Vivo Heart Functional Parameters of Rats by Echocardiography at 72 Hours After Surgery

Heart function	Sham	I/R	I/R-T3
LVEDd (mm)	5.8 ± 0.2	6.0 ± 0.2	5.9 ± 0.2
LVESd (mm)	2.3 ± 0.2	3.3 ± 0.1 [a, b]	2.5 ± 0.2
SAWT %	70 ± 3	52 ± 4 [a, b]	67 ± 3
SPWT %	69 ± 3	63 ± 4	70 ± 2
FS %	59 ± 2	46 ± 2 [a, b]	59 ± 2[b]
HR	437 ± 8	450 ± 16	488 ± 9[a]

[a] $P \leq 0.01$ vs sham.

[b] $P \leq 0.01$ vs I/R-T3.

Values are mean ± SEM; n = 8 in each group.

LVEDd indicates left ventricular end-diastole diameter; LVESd indicates left ventricular end-systole diameter; SAWT% indicates percent systolic anterior wall thickening; SPWT% indicates percent systolic posterior wall thickening; FS% indicates percent of fractional shortening; HR indicates heart rate.

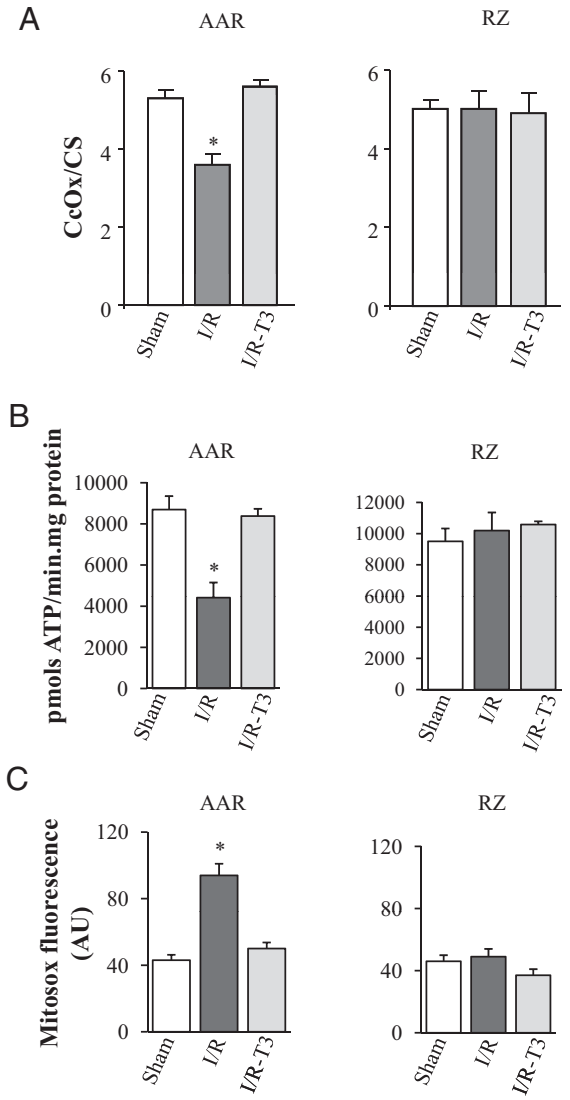

Figure 1. T3 administration rescues mitochondrial activity and limits superoxide formation. At 24 hours after MI, T3 solution at 6 μg/kg/d (I/R-T3), or saline (I/R) were infused for 48 hours. A, The citrate synthase (CS) normalized cytochrome c oxidase (CcOx) activity was measured in the area at risk (AAR) and remote zone (RZ) of the LV. T3 infusion reversed the mitochondrial activity impairment observed in the AAR of I/R group. No differences were assessed in the LV RZ ($n \geq 7$ in each group; *, $P \leq .0001$ vs sham and I/R-T3). B, T3 administration prevents the fall in ATP production rate observed in the AAR of the I/R group whereas no differences among groups were reported in the RZ ($n \geq 4$ in each group; *, $P \leq .0005$ vs sham and I/R-T3). C, Mitochondrial superoxide level was significantly increased in the AAR of the I/R group and return to sham level in the I/R-T3 group. RZ superoxide levels were not affected by ischemia or T3 treatment ($n \geq 4$ in each group; *, $P \leq .0007$ vs sham and I/R-T3).

ings indicate a cardioprotective action of T3 linked to the maintenance of mitochondrial activity and to decreasing apoptosis and necrosis in the early post-ischemic period.

T3 affects the expression and protein level of p53 and prevents mitochondrial permeability transition

In the light of the protective action of T3 from apoptosis and necrosis induced by I/R injury, we then evaluated the role of T3 in the regulation of p53 mRNA and protein level and on p53 downstream events that are Bax activation and mitochondrial inner membrane permeabilization. When compared with the sham group, the I/R group showed increased p53 expression in the AAR (Figure 3A) with a concomitant increase in p53 content (Figure 3B). These alterations were paralleled by an increase in Bax expression and mitochondrial membrane depolarization indicative of apoptosis activation and permeability transition (Figure 3, C and D). These effects were almost completely reverted by T3 administration (Figure 3, A–D). No significant differences between groups were observed in the LV RZ regarding p53 mRNA and protein levels (Figure 3, A and B), Bax expression (Figure 3C), or inner mitochondrial membrane potential (Figure 3D). These findings suggest that p53 mediated proapoptotic and pronecrotic signaling are still detectable in the AAR 72 hours after I/R and can be mitigated by T3 infusion.

p53 modulation by T3 is related to miR-30a upregulation: in vivo and in vitro evidence

miRNAs have emerged as crucial regulators of cardiovascular function and some of them have key roles in cardiac remodeling (8, 9, 11, 12, 17). Given the important contribution of miR-30a in p53 modulation (16), we proceeded by assessing the effect of T3 on the expression of miR-30a in our I/R hearts. As previously reported (17, 18), compared with the sham group miR-30a was downregulated in the AAR of the I/R group (Figure 4A) and T3 was able to limit miR-30a fall (Figure 4A).

No significant differences were observed among groups in miR-30a expression within the RZ (Figure 3A). These data suggest the hypothesis whereby the modulation of miR-30a expression by T3 mediates the inhibitory effects of the hormone on p53 signaling activation and mitochondrial dysfunction in the post-ischemic AAR. In accordance, a significant positive linear regression was found between miR30a levels and mitochondrial function in the I/R groups (Figure 4B).

The mechanistic link between miR-30a and p53 regulation by T3 treatment was explored in primary cultures of neonatal rat CM. Cell cultures were incubated in the presence of 100 nM T3 or saline for 24 hours after being exposed to 24-hour hypoxia. The efficacy of the hypoxic

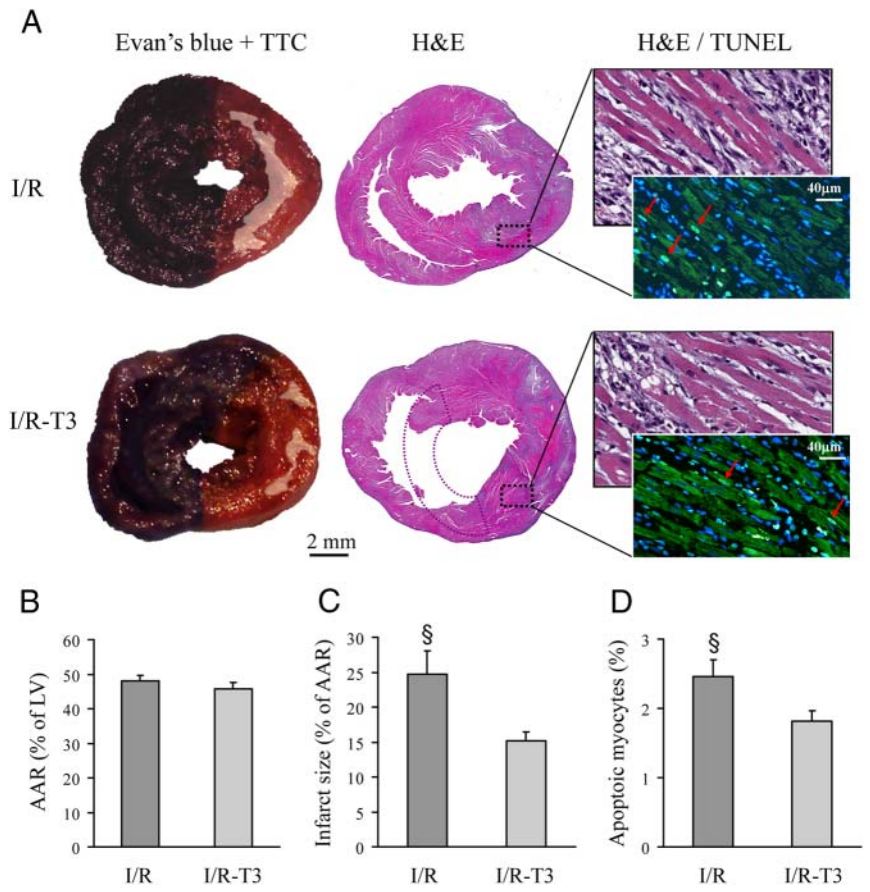

Figure 2. T3 administration improves morphometric parameters and favors cell survival in I/R rat hearts. A, Coronal section of I/R (upper) and I/R-T3 (lower) hearts injected with Evan's blue and incubated with TTC (left), stained with Hematoxylin-Eosin (middle and right) or processed for apoptosis detection by TUNEL fluorescent labeling (right). The black dotted boxes outline the correspondent region at high magnification. Red arrows point to the TUNEL positive green nuclei. Alpha sarcomeric actin was used as a cardio-specific marker (green cytoplasm). Low magnification: 2-mm calibration bar; high magnification: 40-μm calibration bar. B, I/R and I/R-T3 groups presented comparable area at risk (AAR, negative to Evan's blue staining) expressed as percentage of the total LV. C, When compared with I/R, I/R-T3 rats exhibited reduced infarct size expressed as the area within the AAR negative to TTC staining. D, With respect to I/R, IR-T3 showed fewer apoptotic CMs, expressed as the percentage of TUNEL-positive (green) nuclei compared with total nuclei of CMs (both blue- and green-stained nuclei embedded in green cytoplasm). In B, C, and D data are expressed as the mean ± SEM, n = 3 in each group. §, $P <$ .05 vs I/R-T3.

stress was confirmed by the induction of apelin expression (data not shown) (36).

In accordance with the in vivo study, T3 treatment restored miR-30a and p53 levels that were altered by hypoxic stress (Figure 5A–C). miR-30a knockdown (KD) significantly decreased the endogenous miR-30a both regardless of T3 treatment (Supplemental Figure 3).

In addition, in hypoxic conditions, miR-30a KD further increases the p53 level as expected, and, more importantly, completely abolished the T3 mediated effect on p53 expression and protein level (Figure 5, A–C). These data support a model whereby modulation of the miR-30/p53 axis is one of the mechanisms through which T3 may exert a cardioprotective effect.

Discussion

Soon after AMI, a number of neuro-hormonal changes occur with diverse pathophysiological consequences. Among them, decreased levels of T3, the biologically active TH, is frequently observed and there is a long-lasting dilemma as to whether this abnormality needs correction (37). However, growing clinical and experimental findings suggest that THs may be cardioprotective by increasing tolerance of the myocardium to ischemia (28–30, 32, 38). We previously showed that early T3 administration in a rat model of ischemic HF prevented cardiac remodeling and decreased CM death by rescuing mitochondrial function and biogenesis, but the underlying mechanisms are still incompletely understood (32).

Mitochondrial impairment is a leading cause of cell loss and contractile dysfunction in AMI as well as in the subacute and chronic stages of cardiac disease (2, 6). Recovery from the acute injury and subsequent cell death requires inhibition of both necrotic and apoptotic signal pathways.

Here we investigated the mitochondria-targeted regulatory effects of T3 in the early post-ischemic setting by using an experimental model of I/R that closely mimics human AMI disease. Based on previous indications (29, 30, 38), we used a near physiological dose and, to avoid the risk of starting the treatment in presence of unstable cardiovascular and systemic conditions, we started the treatment protocol 24 hours after I/R. A main finding of the present study is that early T3 administration was able to maintain the normal LVFS and proved efficacious in blunting the detrimental effect of I/R on systolic diameter and LV anterior contractility.

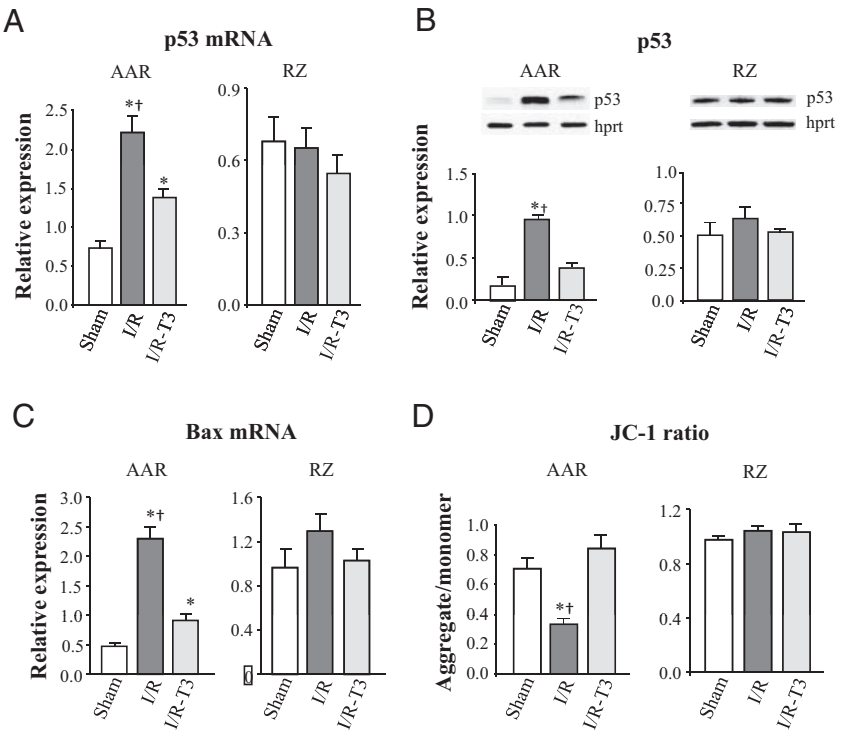

Figure 3. T3 treatment limits p53 upregulation and hampers p53-dependent mitochondrial death signaling in the post I/R setting. A, p53 relative expression was significantly increased in the I/R AAR 72 hours after ischemia and this effect was almost reverted by 48-hour administration of T3. No differences were observed in the RZ B, p53 relative protein content paralleled gene expression in both AAR and RZ. Representative WB is reported in the upper panel; data quantification is shown in the lower panel. C, The 48-hour T3 infusion greatly inhibited the Bax overexpression observed in the I/R AAR. No differences were evidenced in the RZ. D, Mitochondrial inner membrane depolarization was still present 72 hours after ischemia in the AAR of I/R group but not in I/R-T3 group. No alterations of the mitochondrial inner membrane potential were observed in the RZ (n ≥ 5 in each group; *, $P \leq .003$ vs sham, †, $P \leq .0002$ vs I/R-T3).

Looking for a molecular explanation of these physiological results, we found that T3 was able to counteract the upregulation of p53 and its multifaceted adverse effects on mitochondrial activity and cell fate observed in the AAR of the untreated rats. p53 is involved in the regulation of mitochondrial function and dynamics. In fact, at physiological levels, p53 maintains the normal transcription of genes associated with oxidative phosphorylation and the mtDNA copy number (39–40). In contrast, supra-physiological levels of p53 have the opposite effect on mitochondrial integrity and biogenesis (20, 41). In accordance with this, we observed a significant increase of p53 content and elevated superoxide levels in I/R rats associated with decreased cytochrome *c* oxidase activ-

ity and ATP production rate. These alterations were reverted by T3 administration.

Moreover, it is well established that p53 can trigger cell death via apoptosis through the mitochondrial pathway (42). For example, it can transactivate Bax, the proapoptotic member of the BCL-2 family (43). Accordingly, in the AAR of I/R hearts p53 upregulation resulted in stimulation of Bax expression and increase in apoptotic index that were partially reverted by T3 administration. More recently, p53 and Bax have also been recognized as promoters of necrosis through direct and indirect mechanisms that facilitate mitochondrial permeability transition pore opening and lead to inner mitochondrial membrane depolarization that is an important indicator of mitochondrial dysfunction and cell death (19, 44). In our I/R model a depolarization of the inner mitochondrial membrane is still present 72 hours after AMI and is consistent with the activation of p53/Bax pronecrotic axis. T3 infusion prevents mitochondrial depolarization and reduces the extent of cell loss in the AAR, thus resulting in diminished ischemic area/AAR ratio. Overall, our biochemical and molecular findings could explain the better functional recovery observed in the I/R-T3 group.

Given the detrimental effects of p53 signaling in I/R, its repression may be regarded as potentially cardioprotective. miRNAs are important regulators of gene expression, with critical impact on cardiovascular function (45). Reactivation of a fetal miRNA program contributes to the alterations observed in response to diverse cardiac stresses, such as HF and myocardial I/R (46). Of the downregulated miRNAs, the miR-30 family has been reported to play a key pro-survival role through targeting p53 expression (16). Noteworthy, TH is a well-known regulator of myocardium maturation, and T3 decline in heart disease is associated with recapitulation of the fetal expression pattern (11, 47). Hence, we hypothesized that the post-I/R low-T3S might contribute to miR-30 downregulation, thus favoring the observed p53 rise. In line with recent findings (18), here we confirm the early post-I/R downregulation of miR-30a in the AAR and we report for the first time a pivotal contribution of T3 in limiting the post-ischemic drop of miR-30a levels. To strengthen our hypothesis of in vivo connection between T3 and miR-30a levels, rats that did not exhibit the low-T3S after I/R (not enrolled because they did not satisfy the inclusion criteria)

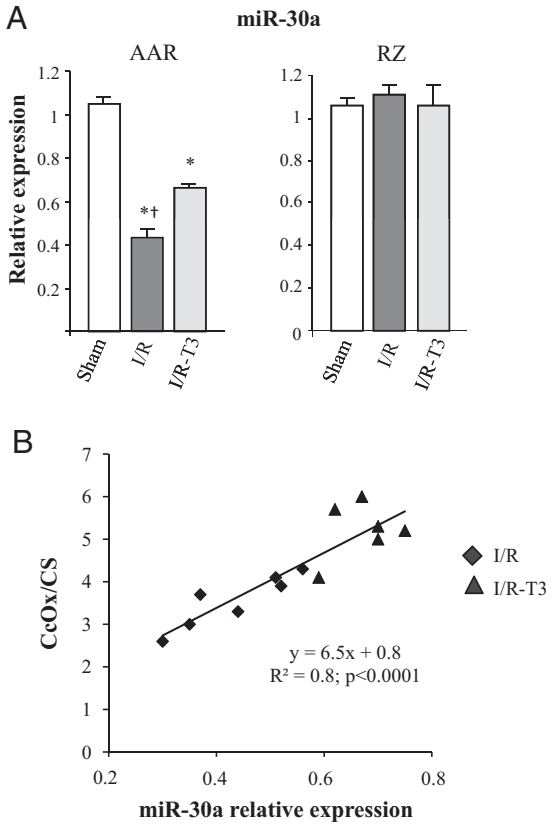

Figure 4. T3 treatment modulates the post I/R expression of miR-30a. A, Forty-eight-hour T3 infusion partially reverted miR-30a level reduction observed 72 hours after ischemia in the I/R AAR. (n ≥ 6 in each group; *, $P \leq .03$ vs sham, †$P \leq .02$ vs I/R-T3). No differences between groups were observed in miR-30a expression levels of the RZ. B, Regression between miR-30a level and mitochondrial function in the AAR of I/R groups.

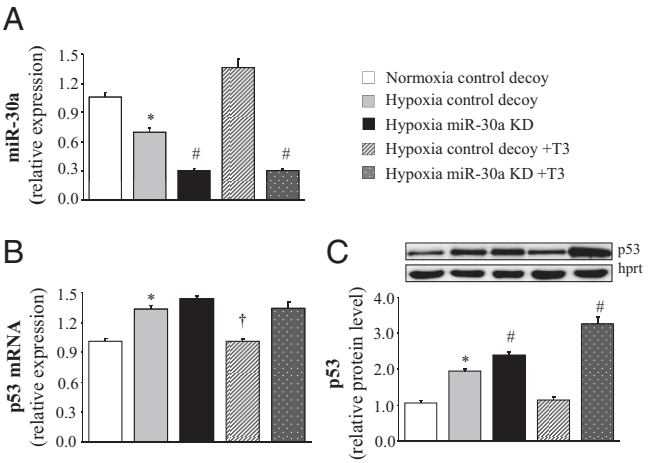

Figure 5. T3 decreases p53 expression and protein levels in cell cultures through downregulation of miR-30a level. Neonatal rat CMs were transfected with miR-30a decoy or control decoy and stressed with 24 hours hypoxia before being exposed to 100 nM T3 or vehicle. Normoxic cell transfected with control decoy served as control. A, In the presence of control decoy T3 treatment induced miR-30a upregulation. miR-30a KD significantly decreased miR-30a level even after T3 stimulation. B and C**,** T3 treatment significantly reduced p53 expression and protein level in cells transfected with control decoy whereas it was ineffective in cells transfected with miR-30a specific decoy. C, Upper panel representative WB; lower panel data quantification. n = 3 in each experimental condition; *, $P \leq .0002$ vs normoxia-control decoy and hypoxia-control decoy + T3; #, $P < .0001$ vs normoxia-control decoy, hypoxia control decoy and hypoxia control decoy + T3; †, $P \leq .0002$ vs hypoxia miR-30 KD and mir30a KD+T3.

showed higher miR-30a levels with respect to the low-T3S I/R group (see Figure 4 Supplemental Data).

Our in vitro data suggest a model linking miR-30a upregulation to the p53 decrease after T3 treatment. As a whole, our findings allow us to hypothesize a new T3-mediated regulatory network for cardioprotection. As depicted in Figure 6, the ischemic condition may favor the decrease of miR-30a levels and the subsequent p53 upregulation. p53, in turn, enhances mitochondrial dysfunction and activates Bax that conveys the p53 proapoptotic and pronecrotic signals, further exacerbating cell loss. T3 treatment may counteract the decrease in miR-30a levels after ischemia, thus limiting the activation of p53 and the pernicious cascade leading to mitochondrial impairment and cell death.

Although the clinical applicability of our approach is far from being practical, the subject of research would have a remarkable impact on translational medicine, as indicated by a recent clinical study reporting that post-ischemic activation of p53 and increased expression of the p53-responsive miRNAs are probably involved in the pathogenesis of HF after AMI (48).

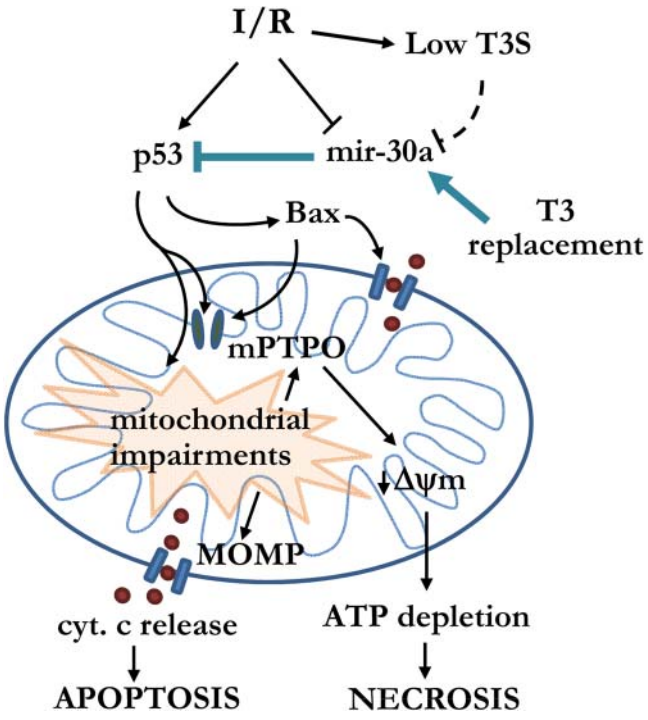

Figure 6. Proposed model for a role of miR-30a in T3-dependent cardioprotection after I/R. In the early I/R setting a decreased T3 level is observed in concomitance with miR-30a downregulation that enhances p53 upregulation. p53 promotes mitochondrial mediated cell death via Bax activation. Through the proapoptotic pathway, Bax prompts mitochondrial outer membrane permeabilization followed by cytochrome c release and apoptosis. Through the pronecrotic pathway Bax signaling leads to mitochondrial permeability pore opening (mPTPO), resulting in a loss of inner mitochondrial membrane potential ($\Delta\Psi$m), ATP depletion and cell death. Moreover, p53 directly enhances the post-ischemic mitochondrial impairments that drive mPTPO and citochrome c release. Near-physiological T3 dose limits I/R injury by maintaining miR-30a level, thus opposing the p53 adverse effects on mitochondrial integrity and cell fate.

A limitation of this study is that also a putative physiological, cardioprotective dose of T3, modifies circulating TH levels (Table 1) and induces a light but significant increase in heart rate (Table 2). Moreover, because the functional study was performed under anesthesia, in our conditions animal sedation might have in part masked the heart rate increase induced by T3. Thus, further investigations will be necessary to define the proper dosage and timing of TH administration.

Secondly, additional dedicated loss-of- or gain-of-function in vivo studies are required to unequivocally prove our hypothesis that miR-30a mediated T3 effects are the main mechanisms opposing post-ischemic adverse ventricular remodeling.

In conclusion, we reported a new T3-modulated cardioprotective pathway which might be exploited to limit mitochondrial impairment and cell loss in the early post-ischemic setting. Our findings support the putative role of T3 treatment in the early post-ischemic phase to hinder adverse ventricular remodeling.

Acknowledgments

We thank Miss Alison Frank for her linguistic revision of the manuscript.

Address all correspondence and requests for reprints to: Dr Giorgio Iervasi, MD, CNR Institute of Clinical Physiology, CNR/Tuscany Region G Monasterio Foundation, Via G. Moruzzi 1, Pisa, Italy; Email: iervasi@ifc.cnr.it.

This work was supported by the Tuscany Region Research Grant (DGR 1157/2011).

Disclosure Summary: The authors have nothing to disclose.

References

1. **Dorn GW 2nd.** Apoptotic and non-apoptotic programmed cardiomyocyte death in ventricular remodelling. *Cardiovasc Res*. 2009; 81:465–473.
2. **Whelan RS, Kaplinskiy V, Kitsis RN.** Cell death in the pathogenesis of heart disease: mechanisms and significance. *Annu Rev Physiol*. 2010;72:19–44.
3. **Baines CP.** The cardiac mitochondrion: nexus of stress. *Annu Rev Physiol*. 2010;72:61–80.
4. **Marín-García J, Goldenthal MJ.** Mitochondrial centrality in heart failure. *Heart Fail Rev*. 2008;13:137–150.
5. **Baines CP, Kaiser RA, Purcell NH, et al.** Loss of cyclophilin D reveals a critical role for mitochondrial permeability transition in cell death. *Nature*. 2005;434:658–662.
6. **Nakayama H, Chen X, Baines CP, et al.** Ca2+− and mitochondrial-dependent cardiomyocyte necrosis as a primary mediator of heart failure. *J Clin Invest*. 2007;117:2431–2444.

7. **Nakagawa T, Shimizu S, Watanabe T, et al.** Cyclophilin D-dependent mitochondrial permeability transition regulates some necrotic but not apoptotic cell death. *Nature*. 2005;434:652–658.
8. **van Rooij E, Sutherland LB, Qi X, Richardson JA, Hill J, Olson EN.** Control of stress-dependent cardiac growth and gene expression by a microRNA. *Science*. 2007;316:575–579.
9. **Barringhaus KG, Zamore PD.** MicroRNAs: regulating a change of heart. *Circulation*. 2009;119:2217–2224.
10. **Divakaran V, Mann DL.** The emerging role of microRNAs in cardiac remodeling and heart failure. *Circ Res*. 2008;103:1072–1083.
11. **Thum T, Galuppo P, Wolf C, et al.** MicroRNAs in the human heart: a clue to fetal gene reprogramming in heart failure. *Circulation*. 2007;116:258–267.
12. **van Rooij E, Marshall WS, Olson EN.** Toward microRNA-based therapeutics for heart disease the sense in antisense. *Circ Res*. 2008; 103:919–928.
13. **Aurora AB, Mahmoud AI, Luo X, et al.** MicroRNA-214 protects the mouse heart from ischemic injury by controlling Ca^{2+} overload and cell death. *J Clin Invest*. 2012;122:1222–1232.
14. **Wang X, Zhang X, Ren X, et al.** MicroRNA-494 targeting both proapoptotic and antiapoptotic proteins protects against ischemia/reperfusion-induced cardiac injury. *Circulation*. 2010;122:1308–1318.
15. **Wang JX, Jiao JQ, Li Q, et al.** miR-499 regulates mitochondrial dynamics by targeting calcineurin and dynamin-related protein-1. *Nat Med*. 2011;17:71–78.
16. **Li J, Donath S, Li Y, Qin D, Prabhakar B, Li P.** miR-30 regulates mitochondrial fission through targeting p53 and the dynamin-related protein-1 pathway. *PLoS Genet*. 2010;6:e1000795.
17. **Duisters RF, Tijsen AJ, Schroen B, et al.** miR-133 and miR-30 regulate connective tissue growth factor: implications for a role of microRNAs in myocardial matrix remodeling. *Circ Res*. 2009;104: 170–178.
18. **Gambacciani C, Kusmic C, Chiavacci E, et al.** miR-29a and miR-30c negatively regulate DNMT3a in cardiac ischemic tissues: implications for cardiac remodeling. *MICRNACR*. 2013;2013:34–44.
19. **Vaseva AV, Marchenko ND, Ji K, Tsirka SE, Holzmann S, Moll UM.** p53 opens the mitochondrial permeability transition pore to trigger necrosis. *Cell*. 2012;149:1536–1548.
20. **Villeneuve C, Guilbeau-Frugier C, Sicard P, et al.** p53-PGC-1α pathway mediates oxidative mitochondrial damage and cardiomyocyte necrosis induced by monoamine oxidase-A upregulation: role in chronic left ventricular dysfunction in mice. *Antioxid Redox Signal*. 2013;18:5–18.
21. **Wrutniak-Cabello C, Casas F, Cabello G.** Thyroid hormone action in mitochondria. *J Mol Endocrinol*. 2001;26:67–77.
22. **Goldenthal MJ, Ananthakrishnan R, Marín-García J.** Nuclear-mitochondrial cross-talk in cardiomyocyte T3 signaling: a time-course analysis. *J Mol Cell Cardiol*. 2005;39:319–326.
23. **Marín-García J.** Thyroid hormone and myocardial mitochondrial biogenesis. *Vascul Pharmacol*. 2010;52:120–130.
24. **Hamilton MA, Stevenson LW, Luu M, Walden JA.** Altered thyroid hormone metabolism in advanced heart failure. *J Am Coll Cardiol*. 1990;16:91–95.
25. **Wiersinga WM, Lie KI, Touber JL.** Thyroid hormones in acute myocardial infarction. *Clin Endocrinol (Oxf)*. 1981;14:367–374.
26. **Friberg L, Drvota V, Bjelak AH, Eggertsen G, Ahnve S.** Association between increased levels of reverse triiodothyronine and mortality after acute myocardial infarction. *Am J Med*. 2001;111:699–703.
27. **Iervasi G, Pingitore A, Landi P, et al.** Low-T3 syndrome: a strong prognostic predictor of death in patients with heart disease. *Circulation*. 2003;107:708–713.
28. **Pingitore A, Galli E, Barison A, et al.** Acute effects of triiodothyronine (T3) replacement therapy in patients with chronic heart failure and low-T3 syndrome: a randomized, placebo-controlled study. *J Clin Endocrinol Metab*. 2008;93:1351–1358.
29. **Henderson KK, Danzi S, Paul JT, Leya G, Klein I, Samarel AM.** Physiological replacement of T3 improves left ventricular function in an animal model of myocardial infarction-induced congestive heart failure. *Circ Heart Fail*. 2009;2:243–252.
30. **Chen YF, Kobayashi S, Chen J, et al.** Short term triiodo-L-thyronine treatment inhibits cardiac myocyte apoptosis in border area after myocardial infarction in rats. *J Mol Cell Cardiol*. 2008;44:180–187.
31. **Pantos C, Mourouzis I, Markakis K, Tsagoulis N, Panagiotou M, Cokkinos DV.** Long-term thyroid hormone administration reshapes left ventricular chamber and improves cardiac function after myocardial infarction in rats. *Basic Res Cardiol*. 2008;103:308–318.
32. **Forini F, Lionetti V, Ardehali H, et al.** Early long-term L-T3 replacement rescues mitochondria and prevents ischemic cardiac remodelling in rats. *J Cell Mol Med*. 2011;15:514–524.
33. **Weltman NY, Ojamaa K, Savinova OV, et al.** Restoration of cardiac tissue thyroid hormone status in experimental hypothyroidism: a dose-response study in female rats. *Endocrinology*. 2013;154: 2542–2552.
34. **Nicolini G, Pitto L, Kusmic C, et al.** New insights into mechanisms of cardioprotection mediated by thyroid hormones. *J Thyroid Res*. 2013;2013:264387.
35. **Bianco AC, Anderson G, Forrest D, et al.** American thyroid association guide to investigating thyroid hormone economy and action in rodent and cell models. *Thyroid*. 2014;24:88–168.
36. **Eyries M, Siegfried G, Ciumas M, et al.** Hypoxia-induced apelin expression regulates endothelial cell proliferation and regenerative angiogenesis. *Circ Res*. 2008;103:432–4015.
37. **Kaptein EM, Beale E, Chan LS.** Thyroid hormone therapy for obesity and nonthyroidal illnesses: a systematic review. *J Clin Endocrinol Metab*. 2009; 94:3663–3675.
38. **Pantos C, Mourouzis I, Saranteas T, et al.** Thyroid hormone improves postischaemic recovery of function while limiting apoptosis: a new therapeutic approach to support hemodynamics in the setting of ischaemia-reperfusion? *Basic Res Cardiol*. 2009;104:69–77.
39. **Matoba S, Kang JG, Patino WD, et al.** p53 regulates mitochondrial respiration. *Science*. 2006;312:1650–1653.
40. **Park JY, Wang PY, Matsumoto T, et al.** p53 improves aerobic exercise capacity and augments skeletal muscle mitochondrial DNA content. *Circ Res*. 2009;105:705–712, 11 p following 712.
41. **Hoshino A, Mita Y, Okawa Y, et al.** Cytosolic p53 inhibits Parkin-mediated mitophagy and promotes mitochondrial dysfunction in the mouse heart. *Nat Commun*. 2013;4:2308.
42. **Vousden KH.** p53: death star. *Cell*. 2000;103:691–694.
43. **Miyashita T, Reed J.** Tumor suppressor p53 is a direct transcriptional activator of the human bax gene. *Cell*. 1995;80:293–299.
44. **Whelan RS, Konstantinidis K, Wei AC, et al.** Bax regulates primary necrosis through mitochondrial dynamics. *Proc Natl Acad Sci USA*. 2012;109:6566–6571.
45. **Bauersachs J, Thum T.** Biogenesis and regulation of cardiovascular microRNAs. *Circ Res*. 2011;109:334–347.
46. **Ye Y, Perez-Polo JR, Qian J, Birnbaum Y.** The role of microRNA in modulating myocardial ischemia-reperfusion injury. *Physiol Genomics*. 2011;43:534–542.
47. **Pantos C, Mourouzis I, Cokkinos DV.** Thyroid hormone and cardiac repair/regeneration: from Prometheus myth to reality? *Can J Physiol Pharmacol*. 2012;90:977–987.
48. **Matsumoto S, Sakata Y, Suna S et al.** Circulating p53-responsive microRNAs are predictive indicators of heart failure after acute myocardial infarction. *Circ Res*. 2013;113:322–326.